UNIZIK JOURNAL OF ENGINEERING AND APPLIED SCIENCES (UJEAS)

Research Article

Process Optimization of Zinc Chloride Activated Carbon Production from Avocado Pear Seed Waste: An Assessment of Artificial Neural Network and Box-Behnken Design

Karinate Valentine Okiy, Joseph Tagbo Nwabanne

Special Issue

A Themed Issue in Honour of Professor Clement Uche Atuanya on His retirement.

This themed issue pays tribute to Professor Clement Uche Atuanya in recognition of his illustrious career in Metallurgical and Materials Engineering as he retires from Nnamdi Azikiwe University, Awka. We celebrate his enduring legacy of dedication to advancing knowledge and his impact on academia and beyond through this collection of writings.

Edited by
Chinonso Hubert Achebe PhD.
Christian Emeka Okafor PhD.

UNIZIK JOURNAL OF ENGINEERING AND APPLIED SCIENCES

UNIZIK Journal of Engineering and Applied Sciences 3(3), September (2024), 1016-1036
Journal homepage: https://journals.unizik.edu.ng/index.php/ujeas
PRINT ISSN: 2992-4383 || ONLINE ISSN: 2992-4391

Process Optimization of Zinc Chloride Activated Carbon Production from Avocado Pear Seed Waste: An Assessment of Artificial Neural Network and Box-Behnken Design

Karinate Valentine Okiy [1*], and Joseph Tagbo Nwabanne [2]
[1]Department of Chemical Engineering, Faculty of Engineering, Nnamdi Azikiwe, Nigeria.
[2]Department of Chemical Engineering, Faculty of Engineering, Nnamdi Azikiwe, Nigeria.
[*]Corresponding Author's E-mail: karinateokiy@gmail.com

Abstract
This study deals with the production of avocado pear seed activated carbons using acidic (sulphuric acid) reagent according to Response Surface Methodology (RSM) and Machine learning (ML) approaches. During the investigation, Artificial neural network (ANN) and Box Behnken Design (BBD) were used to assess the influence of the activation temperature (600 -900^{0}C), activation time (60-120 mins), and impregnation ratio (0.5-1.5) on the achievable BET surface area. The optimization of sulphuric acid-activated avocado pear seed production was also comparatively examined using both BBD with the RSM approach and ANN neural network model to determine the optimum process conditions. The Analysis of Variance (ANOVA) unveiled that the significant factors were activation temperature, and impregnation ratio for the avocado pear seed acid activation process, as all their p-values were less than 0.1. The best process conditions discovered for producing optimal BET surface area of H2SO4 activated carbon were activation temperature (1045.73K), activation time (120mins), and impregnation ratio (1.21) respectively. The optimal BET surface area achieved for H_2SO_4-activated avocado pear seed (APS) was 517.8m^2.g^{-1}. The correlation coefficient (R) for the RSM and ANN BET models were found to be 0.88, and 0.9955 respectively. Based on these results, the ANN BET model was ascertained to be the most capable model for predicting and forecasting the achievable surface area of H_2SO_4-activated avocado pear seed (APS). The RSM and ANN neural network can be applied as effective analytical tools for optimizing the HAPS production process.

Keywords: Box Behnken Design; Acid activation; Low-cost agro wastes derived adsorbents; Artificial Neural Networks (ANN); Error Analysis.

1. Introduction

Globally, the rapid rise in human population is leading to increased stresses on available clean water resources. Increasing urbanization and industrialization activities are resulting in the release of huge quantities of contaminated effluents into surface water bodies, that infiltrate into the groundwater (aquifer), which is the major source of fresh-water supply (Bodzek *et al.* 2020). Clean drinking water is becoming more and more limited in supply, partly due to the rapid increase in global population, and pollution of surface/groundwater systems as a result of man-made (anthropogenic) activities (Jafarinejad, 2017). It is estimated that 4-5 billion of the world's population will inhabit regions without access to fresh and clean water supply (Ali *et al.* 2016). Noteworthy, about 80% of diseases affecting mankind can be traced to poor drinking water quality. This mostly endangers the lives of people residing in the developing world (Muller *et al*. 2020). Thus, it is necessary that water emanating from major industrial and municipal sources of pollution is properly treated to ensure that their effluent discharges meet environmental legislation and standards to protect human health and the environment.

Several treatment technologies exist for wastewater decontamination including membrane separation, electro-deionization, evaporation, coagulation and flocculation, reverse osmosis, filtration, flotation, chemical precipitation, and adsorption (Howard *et al.* 1986). The adsorption method is highly preferred due to its inherent advantages of low cost, high efficiency, simplicity of design, ease of operation, number of available sorption sites and chemical reactivity of the adsorbent material(s) (Malik *et al.* 2016). The main classes of adsorbents include natural, synthetic and semi-synthetic. The natural adsorbents are lignocellulosic materials such as leaves, plants and agricultural waste used for treatment of real or simulated wastewater, they are inexpensive but have low to medium adsorption capacities. While, synthetic adsorbents are produced using established laboratory methods, these porous material have enhanced adsorptive properties (adsorption capacities). However, their manufacturing costs are high. Semi-synthetic adsorbents are prepared using activation processes with or without reagents to develop a finely ordered crystalline structure (high porosity). These adsorbents are derived from natural materials such as agricultural wastes and have advantages of high efficiency, low production costs and possibility of sorbent regeneration (Ali *et al.* 2016). In practice, the adsorption method is implemented using synthetic adsorbents. In recent times, efforts are being made to prepare and utilize semi-synthetic adsorbents derived from agricultural waste such as avocado pear seeds for wastewater treatment, due to the high manufacturing costs of synthetic (commercial) adsorbents (Ighalo *et al.* 2022).

The Avocado (Persea americana) tree is indigenous to Mexico and Central America, but they also thrives in subtropical and tropical climates throughout the world. In Nigeria, avocado trees are cultivated in various regions, including the southern and southwestern parts of the country. Some of the avocado pear varieties grown in Nigeria include Nabal, Fuerte, Hass, and Pinkerton. Avocado pears are used in various dishes, including salads, sandwiches, smoothies, and as a spread on bread or toast. The edible portion of the avocado pear seed is the fleshy part, which is consumed in huge amounts due to its delicious taste and versatility in various culinary applications. Whilst, the large quantities of disposable avocado pear seeds produced are of limited domestic and culinary value, contributing immensely to organic (biodegradable) waste accumulation with the associated waste management problem. Noteworthy, conventional methods for disposal of waste avocado seeds such as recycling and composting are still in their nascent stages in Nigeria. Attempts to produce low-cost activated carbons from waste avocado seeds for utilization in the remediation of contaminated effluents can thus prove to be effective in waste minimization. To date, the preparation of active carbons from raw avocado pear seeds utilizing common activating agents (i.e. sulphuric acid) has been seldom explored (Ighalo *et al.* 2022).

Industrially, activated carbons are characterized in terms of their BET surface area(s) (Dyk., 2000). Notably, the production of good-quality activated carbons with high BET surface area(s) is influenced by several process variables including activation temperature, activation time, and impregnation ratio (Iheanancho *et al*. 2019). Conduction of experimental studies for screening of the optimally activated carbons can be time-consuming, expensive, and labour intensive. Thus, assessment of the effect of operating parameters on geometric attributes (BET Surface area) necessitates the use of data-driven tools such as Response Surface Methodology (RSM) and Artificial Neural Networks (ANN).

RSM is a collection of statistical and mathematical methods that are expedient for the modeling and analysis of problems in which a response of interest is influenced independently and conjunctively by several variables and the aim is to optimize the response (Montgomery, 2017). The major objective of Response Surface Methodology is the sequential use of experimental designs to locate the region in the factor space (response surface) that satisfies the operating requirements (optimal response) (Nooshin & Hamid, 2017). Box Behnken is one of the most prominent experimental designs for RSM compared to Central composite design (CCD), Taguchi, and three-level full factorial designs. The Box Behnken design is a three-level factorial design utilized in RSM for fitting response (quadratic) surfaces. These designs are created by combining incomplete block design with 2 level factorial designs (Okewale *et al*. 2015). The Box Behnken (BBD) design is ideal for a few (3 or 4) experimental factor(s) investigations, as minimal experimental runs are needed with the attendant reduction in physical labour and, consequently lower costs (Montgomery, 2017). According to Melvin *et al*. (2015), the Box Behnken design is well suited for fitting a response surface. Statistical methods such as RSM are effective for rapid analysis and interpretation of robust and well defined dataset(s). However, RSM tends to be unreliable in handling noisy and poor quality data, require multiple parameter(s) for model development and can be difficult to implement for complex real-life processes (Chebii *et al*. 2022). ANN mimics the process of biological neural systems like human intellect in describing the behavior of complex non-linear systems. ANN originated in 1943 by Psychiatrist Warren McCulloch and Logician Walter Pits of the University of Chicago, USA (McColluch & Pits, 1943). Artificial neural network (ANN) is a powerful computational technique with the ability to detect complex patterns in dataset(s) that may not be properly delineated by statistical methods or conceptual models and also has low computational demands (Chebii *et al*. 2022). ANN examines the cause-effect correlation(s) between independent (input) and dependent (output) variables of a given dataset, iteratively updating the network parameters (weights) until the error criterion (minimum MSE) is satisfied. ANN has benefit of exceptional ability to model complex non-linear systems, where changes in system output(s) and associated input(s) are non-proportionate without prior knowledge of the underlying physical phenomena (Li *et al*. 2017). Notwithstanding, ANN modeling still has a number of downsides including slow trial & error process of efficient neural network design (i.e. specification of hidden layers) and model over-fitting (poor generalization) issues.

Previously, RSM has been successfully applied for the modeling and analysis of activated carbon production processes (Mohammed *et al*. 2014; Iheanacho *et al*. 2019). ANN has also been applied in the preparation of nanoadsorbent(s) for wastewater treatment (Bhowmik *et al*. 2016). To the best of our knowledge, ANN and RSM respectively have never been utilized for assessment of the acid (H2SO4) activation of raw avocado pear seeds. This marks the first time that RSM and ANN analytical tools have been applied to comparatively analyze the production of activated carbon from avocado pear seeds with chemical activation (H2SO4). Computer-aided synthesis of porous adsorbent materials such as H2SO4 activated avocado pear seed (HAPS) utilizing data-driven models (i.e. ANN and RSM) have not been carried out before. Thus, the optimization of acid activated avocado pear seeds to maximize the achievable BET surface area of the produced carbons using both ANN and RSM technique(s) constitutes a novel research direction. Pertinently, RSM and ANN algorithms have never been employed applied to identify the optimality location in the design space (region of interest) of the acid (H2SO4)/APS system to facilitate process optimization. Consequently, this work aims to (i) investigate the effective production of activated carbons from avocado pear seeds with acid activation (H2SO4) (ii) select optimal avocado pear seed activated carbons with maximum BET surface areas based on RSM (BBD) design (iii) utilize ANN technique for optimizing the preparation of H2SO4 activated avocado pear seed carbons under different production conditions of activation temperature, time and impregnation ratio (iv) comparatively analyze the performances of the created RSM and ANN BET models to ascertain their efficiencies in predicting the quality of the produced carbons in terms of BET surface area.

2.0 Material and methods

2.1 Activated carbon preparation

The pristine Avocado pear seeds were procured from Eke-Awka market at Awka South Local Government Area, Anambra State in the Eastern part of Nigeria (N: 6^0 13' 8''; E: 7^0 5' 13''). Chemical activation of the avocado kernel seed sample with sulphuric acid as a reagent was performed according to the acid activation procedure reported by Zarzour *et al*. (2014) and Zhu *et al.* (2016) with minor modifications. The experimental procedure for producing the avocado pear seed activated carbon is presented in Figure 1. 300 grams of raw avocado pear seed sample was pre-treated by washing with 5000 grams of distilled water and 3945 grams of ethanol to remove dirt and other soluble impurities. Consequently, the washed avocado pear seed samples were dried in a Mermmert oven at a temperature of 383 K for 24 hours. Then, the dried avocado pear seed samples were cut and ground into fine particles utilizing a Jencod grinding machine and sieved using a standard Taylor Sieve with a mesh size of 300 µm. Thereafter, 300 grams of dried avocado pear seed was mixed with 119.7 grams of 85% sulphuric acid according to the impregnation ratios (0.5:1, 1:1, and 1.5:1) for a total duration of 2 hours and heated in a Mermmert oven at 368 K for 24 hours. The dried acid-impregnated avocado pear samples were then thermally activated in a Muffle furnace at different activation temperatures (873 K, 1023 K, and 1173 K) and times (60, 90, and 120 minutes). The activated carbon sample was cooled, and repeatedly washed to remove disorganized carbon, products of decomposition, and traces of sulphuric acid. The washed activated carbon sample was filtered with Whatman No.1 filter paper and dried in a Mermmert oven at 348 K for 24 hours before usage. Textural characterization of the activated carbon product was performed using a Quantachrome NOVA4200e BET Analyzer (Anton-Paar GmbH, Austria) to determine the BET surface area.

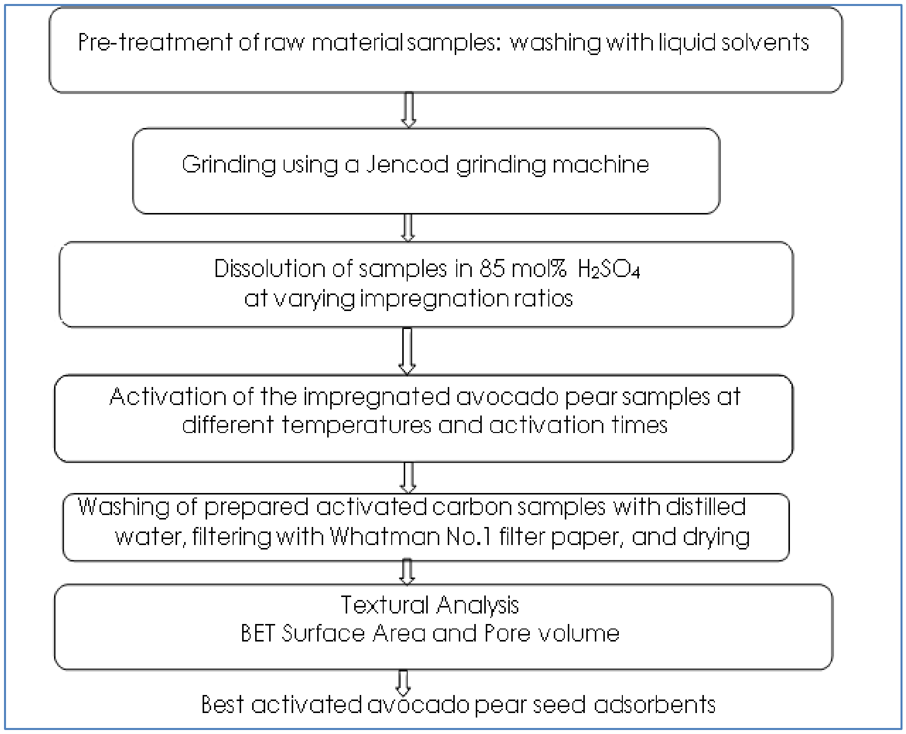

Figure 1: Flowchart showing the method of producing sulphuric acid activated carbon from avocado pear seeds.

2.2. Factorial experimental design by Box Behnken (BBD) Modeling

Response Surface Methodology was utilized as the statistical modeling technique to (i) evaluate the effects of individual factors on the response of interest, (ii) resolve the two-factor interaction effects of the independent variables, and (iii) optimize the achievable BET surface area of sulphuric acid activated avocado pear seed carbon (Anderson & Whitcomb, 2016). The RSM optimization strategy for the APS activated carbon production process was evaluated with the aid of Box Behnken Design (BBD). In this study, the independent variables selected for analysis were activation temperature, impregnation ratio, and activation time. The independent or response variable chosen was BET surface area. The upper and lower limits of the independent variables selected for the BBD are shown in Table 1. The experimental ranges were selected based on prior literature studies (Buasri *et al.* 2023).

For the BBD experimental design, the total number of experimental runs was determined using Eqn.1.

$$N = K^2 + K + + C_P \quad (1)$$

Where N is the number of experimental runs, K is the factor number and C_P is the replicate number of the central point (Melvin *et al.* 2015).

A 3-level, 3-factor Box Behnken Design (BBD) of 48 experimental runs for a combined 2^2 core designs with incomplete block designs (IBD) and 6 centre (median) points leading to a total of 54 experimental runs was adopted, as presented in Table 2. The core points gave an equal variation of the high and low values, whilst the median points ensured reproducibility of the data and gave an estimate of experimental error (Onu *et al.* 2021).

The statistical analysis was carried out using Design Expert Software version 13 (Stat-Ease Inc, USA) to predict the response of the studied system. The 54 experimental trials were carried out in a randomized way to minimize systematic error by adjusting the values of the independent (process) variables in abidance with the design of experiments (DOE).

Table 1: Independent variables and their levels for Box Behnken experimental design.

Independent Variable(s)	**Range and Level**		
	-1	0	+1
Activation temperature (A, ^{0}C)	600	750	900
Activation time (B, mins)	60	90	120
Impregnation ratio (C, Activating agent: raw material)	0.5	1.0	1.5

Box Behnken scheme being a spherical design consists of experimental factors (points) lying at the centre and midpoint of the edges of a sphere of defined radius (Ajemba, 2012; Montgomery, 2017). The independent variables were coded for low, medium, and high settings, as -1, 0, and +1 and evenly spaced (Anderson & Whitcomb, 2016) as shown in Table 1.

Table 2: Box behnken experimental design matrix for chemical activation of avocado pear seed using sulphuric acid.

Run order	**Activation Temp (^{0}C)**	**Activation Time (Mins)**	**Impregnation ratio Activating agent: raw material**	**BET Surface Area (m^2/g)**
1	600	60	1.0	418.3
2	900	60	1.0	434.9
3	600	120	1.0	463.4
4	900	120	1.0	485.1
5	600	90	0.5	215.9
6	900	90	0.5	450.0
7	600	90	1.5	456.1
8	900	90	1.5	464.9
9	750	60	0.5	464.9
10	750	120	0.5	468.5
11	750	60	1.5	471.3
12	750	120	1.5	475.1
13	750	90	1.0	407.1
14	750	90	1.0	407.1
15	750	90	1.0	407.1
16	600	60	1.0	418.3
17	900	60	1.0	434.9
18	600	120	1.0	463.4
19	900	120	1.0	485.1
20	600	90	0.5	215.9
21	900	90	0.5	450.0
22	600	90	1.5	456.1
23	900	90	1.5	464.9
24	750	60	0.5	464.9
25	750	120	0.5	468.5
26	750	60	1.5	471.3
27	750	120	1.5	475.1
28	600	60	1.0	418.3
29	900	60	1.0	434.9
30	600	120	1.0	463.4
31	900	120	1.0	485.1
32	600	90	0.5	215.9
33	900	90	0.5	450.0
34	600	90	1.5	456.1
35	900	90	1.5	464.9
36	750	60	0.5	464.9
37	750	120	0.5	468.5
38	750	60	1.5	471.3

39	750	120	1.5	475.1
40	600	60	1.0	418.3
41	900	60	1.0	434.9
42	600	120	1.0	463.4
43	900	120	1.0	485.1
44	600	90	0.5	215.9
45	900	90	0.5	450.0
46	600	90	1.5	456.1
47	900	90	1.5	464.9
48	750	60	0.5	464.9
49	750	120	0.5	468.5
50	750	60	1.5	471.3
51	750	120	1.5	475.1
52	750	90	1.0	407.1
53	750	90	1.0	407.1
54	750	90	1.0	407.1

Furthermore, the reduction empirical model describing the H2SO4-APS production process can be represented by the following second-order approximating polynomial model equation, in terms of coded factors:

$$Y = b_0 + \sum_{i=1}^{n} b_i X_i + \sum_{i=1}^{n} b_{ii} X_i^2 + \sum_{i=1}^{n-1}\sum_{i=2}^{n} b_{i,j} X_i X_j + E \qquad (2)$$

Where Y is the predicted dependent variable, b_0 is the constant coefficient (intercept), b_i, b_{ij} and b_{ii} are the regression coefficients of the linear, and interaction terms respectively, n is the number of patterns, X_i, and X_j are the independent factors studied, i and j are index numbers, and E is the error term.

2.3. Artificial Neural Network

The artificial neural network (ANN) is a non-linear mathematical mapping of the region between the numeric inputs and output dataset(s) to identify an appropriate generalization of the actual system (Basu, 2013). The ANN training process involves the following steps: (i) initialization of network parameters (weights) (ii) utilization of current weights and biases with nodal activation function(s) to generate an output signal(s) (iii) comparison of the resulting output signal(s) with target output to determine network prediction error(s) (iv) iterative adjustment of network weights from the output unit back to the colligated hidden layer(s) using the back-propagation training algorithm until minimum value of the error function (MSE) is reached.

In this study, the MLP feed-forward network model for predicting the achievable BET surface area of H2SO4-activated APS was created using MATLAB R2018a version 9.4 (MathWorks Inc, USA). The Multi-Layer Perceptron (MLP) feed-forward network with back-propagation (BP) training algorithm was utilized in estimating connections amongst a group of observations, between specific parameters (target variables), and the remainder of the dataset (Chebii *et al*. 2022). Process parameters such as activation temperature, activation time, and acid impregnation ratio, were selected as input (independent) variables to the neural model. In addition, the BET surface area was selected to be the response (dependent) variable. The multi-layer perceptron network is known to perform well when used for modeling non-linear and noisy data (Chebii *et al.* 2022).

The described ANN consists of one input layer, two hidden, and one output layer (Figure 2). The ANN model with two hidden layer architecture was preferred in this case, due to superior results in comparison to ANN with a single hidden layer (Jerry, 2002). The constructed ANN network employed linear transfer function (Purelin) to model the neurons in the network input and output layers respectively, and tangent sigmoid transfer function (Tansig) for the neurons in the hidden layer(s).

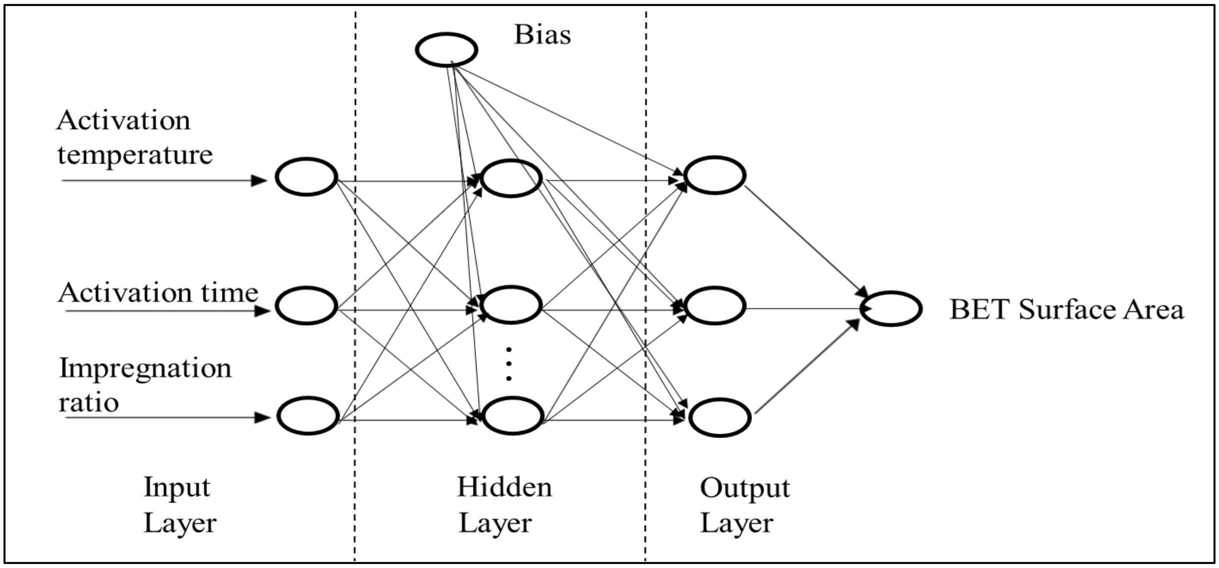

Figure 2: Artificial Neural Network architecture for modeling the APS acid activation process.

To prevent over-fitting, the number of neurons in the hidden layers was estimated based on the following empirical equation [Eqn.3]:

$$\text{Number of hidden neurons} = {}^{1}/_{2} \times (\text{inputs} + \text{outputs}) + \sqrt{(\text{training patterns})} \qquad (3)$$

Where, training patterns are the total number of data points (Basu., 2013).

Based on the result, 9 neurons were chosen as the appropriate number of nodes to be embedded in the hidden layer(s) of the ANN models.

According to Onu *et al.* 2021, ANN modeling fares better with a larger number of dataset(s). Consequently, the experimental dataset for avocado pear seed activation was quadrupled, providing a total of 54 data points utilized for the ANN modeling, of which 70% (38 records) were used in the refinement of network weights and biases (training), 15% (8 records) were used for randomly checking network predictions to assess extrapolation (generalization) performance (validation), and the remaining 15% (8 records) were used for calibration and assessment of network quality (testing). The ANN network (3:5:4:1) incorporating three input variables (activation temperature, activation time, and impregnation ratio), ten (9) hidden neurons, and one (1) performance variable (BET surface area) was ascertained to be suitable for estimating the achievable BET surface area(s) of H2SO4 activated avocado pear seed (See Figure 3).

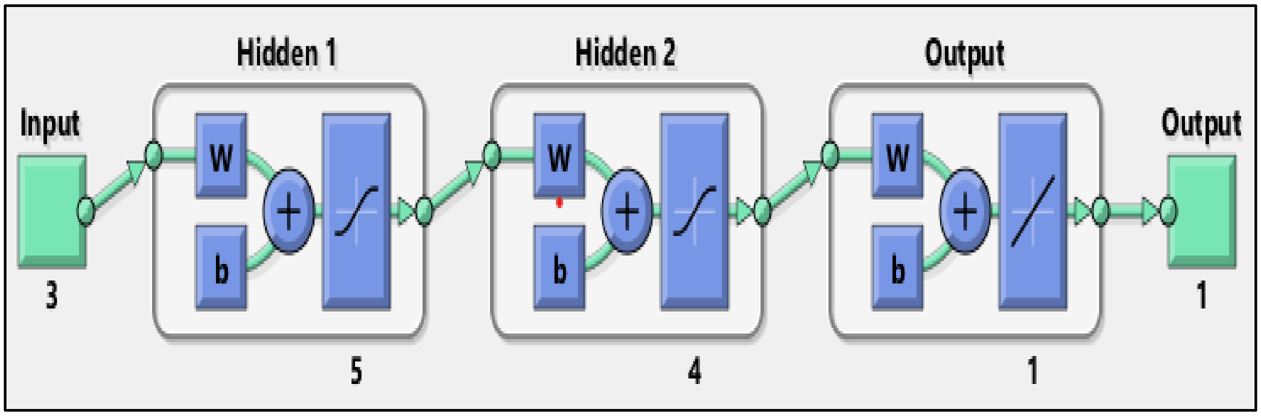

Figure 3: Topology of ANN BET network with 9 hidden neurons.

The ANN model training was carried out using a neural network code, which automates the network training process.

3.0 Results and Discussions

3.1. Modeling of the HAPS activation process using RSM

The Box Behnken design was utilized in a total of 54 experimental runs to develop a correlation between the APS seed-derived activated carbon production variables and BET surface area. According to the Sequential Model Sum of Squares (SMSS), the most suitable model for the activation process was selected based on the highest order polynomial, where the significance probability value (P-value) is less than 0.5 and the Fischer variation ratio (F-value) obtained from Model summary statistics (See Table 3) is greater than the critical F-value [From F-distribution table] (Montgomery., 2017). Thus, the quadratic model was suggested by Design Expert Software for optimizing the achievable BET surface areas of produced H2SO4-activated carbons. However, the cubic model was aliased because the BBD does not hold enough runs to support a cubic model (Onu *et al*. 2021).

Table 3: Sequential model sum of squares analysis [Type 1] for H2SO4-activated avocado seed.

Source	Sum of Squares	df	Mean Square	F-value	P-value	
Mean	$1.024E^{+07}$	1	$1.024E^{+07}$			
Linear	86009.33	3	28669.78	9.31	<0.0001	
2FI	50784.14	3	16928.71	7.78	0.0003	
Quadratic	46020.78	3	15340.26	12.19	<0.0001	Suggested
Cubic	54099.99	3	18033.33			Aliased
Residual	0.0000	40	0.0000			
Total	$1.048E^{+07}$	54	$1.940E^{+05}$			

For assessment of the significance and adequacy of the second-order approximating polynomial model, the Analysis of Variance (ANOVA) for Box Behnken experimental design was applied. The goodness of fit of the second-order approximating polynomial model was assessed using the coefficient of determination R^2, Adjusted R^2, Coefficient of Variation (C.V), Adequate precision, and Standard deviation (SD). Employing the 95% significance level, if the P-value is less than 0.05 and the F-values obtained from the ANOVA Table are greater than the critical F-values then it is safe to conclude that the effect under consideration is significant. The final model for the response was obtained by retaining only the significant factors ($P < 0.05$) based on the F-test. The results of the ANOVA analysis for the H2SO4-activated carbons are shown in Table 4.

Table 4: ANOVA analysis for sulphuric acid activated carbon.

Source	Sum of Squares	Df	Mean Square	F-Value	P-Value
Model	1.828E+05	9	20312.92	16.15	< 0.0001
A-Act. Temp	85514.08	1	85514.08	67.97	< 0.0001
B-Act. Time	3502.08	1	3502.08	2.78	0.1025
C-Impreg. Ratio	6904.52	1	6904.52	5.49	0.0238
AB	26.01	1	26.01	0.0207	0.8863
AC	50760.09	1	50760.09	40.35	< 0.0001
BC	0.0400	1	0.0400	0.0000	0.9955
A^2	7230.99	1	7230.99	5.75	0.0209
B^2	3231.19	1	3231.19	2.57	0.1164
C^2	1516.55	1	1516.55	1.21	0.2784
Residual	54099.99	43	1258.14		
Std. Dev= 35.47	**R-Sqr** = 77.16%	**R-Sqr(Adj)**= 72.39%	**Adeq Precision** = 15.28	**C.V.%**= 8.14	

The predicted response for BET surface area of H2SO4 activated avocado pear seeds (APS) is represented by the following response surface equation [Eqn. 4], accounting for curvilinear effects:

$$\text{BETArea} = -1290.74 + 3.89\times A - 5.66\times B + 824.88\times C + 0.000283\times A\times B - 0.751\times A\times C + 0.00333\times B\times C - 0.001951\times A^2 + 0.0326\times B^2 - 97.45\times C^2 \quad (4)$$

From the ANOVA for H2SO4-APS shown in Table 4, it was observed that the P-value for the response surface model was less than 0.05 (p-value = <0.0001). This indicates that the Second-order polynomial model is significant at the 95% confidence level. Likewise, the evaluated Fisher's F-ratio of 16.15 implied that the response model was significant, with the likelihood of 0.009% that the F-value occurs due to noise, thus confirming the p-value test (Anderson & Whitcomb., 2016; Montgomery, 2017). Also, from the summary of analysis results shown in Table 4, it can be concluded that the linear effects, Activation temperature (A), Impregnation ratio (C), the 2-way interaction A*C (Activation temperature and Impregnation ratio) and square effect, A*A (Activation temperature product) for H2SO4-activated APS had a statistically significant effect on the response, as all their p-values were not greater than 0.1 (Montgomery., 2017). On the other hand, the linear effect B (Activation time), the 2-way interactions A*B (Activation temperature and Activation time), B*C (Activation time and Impregnation ratio) and the square effect, B*B (Activation time product) and C*C (Impregnation ratio product) for H2SO4 activated APS were found to be insignificant as their P-values were greater than 0.1 (Montgomery, 2017).

Likewise, the F-tests for the significance of all the linear, square, and interaction terms in the second-order polynomial model equation confirmed the results of the P-value test (Onu *et al*. 2021). Therefore, the conclusion can be reached that activation temperature and impregnation ratio were the linear terms with the most significant effect(s) on achievable BET surface area of H2SO4-APS, whilst the 2-way interaction of activation temperature and impregnation ratio exhibited the more significant effect on achievable BET surface area for the interactive terms. Normally, as the activation temperature increases, new pores are created in the process, the BET surface area is also increased and the existing pores are subsequently enlarged at significantly higher activation temperatures (Marsh & Rodríguez-Reinoso, 2006). As a result, a positive effect on the textural features (BET surface area, pore volume) of H2SO4 activated avocado pear seed carbon followed with increment in activation temperature of the process. Likewise, the impregnation (mixing) ratio is directly correlated with BET surface area. Impregnation of carbonaceous materials with chemicals creates unsaturated compounds composed of non-carbon elements (heteroatoms) such as oxygen, and hydrogen (surface functional groups) in the end caps and pore walls of the carbon matrix, which enhances the adsorptive capacity of the H2SO4-activated avocado pear seed carbon. Thus, a positive effect on the geometric properties (BET surface area, pore volume) of solid carbon followed with the increase in the impregnation ratio between the activating agent (e.g. sulphuric acid) and raw avocado pear seed (Marsh & Rodríguez-Reinoso, 2006). Consequently, eliminating all the insignificant terms, the final second-order polynomial equation is obtained as:

$$\text{BETArea} = -1290.74 + 3.89\times A + 824.88\times C - 0.751\times A\times C - 0.001951\times A^2 \quad (5)$$

The antagonistic and synergistic effects on achievable BET surfaces of the H2SO4-activated APS are shown by the negative and positive signs in front of the model equation terms.

Table 4 also lists the values of the statistical measures, coefficient of determination R^2 (77.16%), Adjusted R^2 (72.39%), Standard deviation (35.47), Coefficient of Variation C.V. (%) (8.14), and Adequate precision (15.28) used to evaluate the goodness of fit of the second-order polynomial model. The good R^2 statistic ($R^2 > 67\%$) showed that approximately 77.16% of the fluctuations in the response could be attributed to the independent variables studied, with a 0.5% chance that the variations in achievable BET surface area(s) are due to noise, suggesting that the model is adequate at 95% confidence limit (Singh *et al*. 2014). Furthermore, the standard deviation of the second-order polynomial was high, the smaller the standard deviation, and the closer the R^2 value to 1, the better the predictive ability of the polynomial model. The high value of the standard deviation implied a significant amount of variation in the independent variables studied. Likewise, the adequate precision ratio of 15.28, which is greater than 4.0 (desirable value), indicates adequate signal (high signal-to-noise ratio). This implies that the response model can be used to navigate the design space (Anderson and Whitcomb, 2016). According to Okpe *et al*. 2018, an adequate precision ratio greater than 4 indicates that the model is adequate. The coefficient of variation (C.V.) is defined as the ratio of the standard deviation of the estimate to the mean value of the response and is a measure of the repeatability and reproducibility of the model. The evaluated C.V value of 8.14, which was less than 10% (Upper threshold limit) indicates that the response surface model can be considered fairly reproducible (Onu *et al*. 2021). Further, the reasonably close agreement of the R^2 value of 77.16% and adjusted R^2 value of 72.39% (difference < 20%) confirms the adequacy of the regression model. The results of the predicted response and experimental response are shown in Table 5.

Table 5: Model predicted and experimental BET surface area for H_2SO_4 activated APS.

Point	BET Surface Area (Predicted)	BET Surface Area (Actual)	STD Error Fit	Square Residual
1	403.712	418.3	0.46153	212.81
2	471.462	434.9	-1.15678	1336.78
3	426.837	463.4	1.15678	1336.85
4	499.688	485.1	-0.46153	212.81
5	271.738	215.9	-1.76662	3117.88
6	454.687	450.0	-0.14831	21.968
7	451.412	456.1	0.14831	21.977
8	409.062	464.9	1.76662	3117.88
9	423.650	464.9	1.30509	1701.56
10	449.225	468.5	0.60983	371.53
11	490.575	471.3	-0.60983	371.53
12	516.350	475.1	-1.30509	1701.56
13	407.100	407.1	0.00000	0
14	407.100	407.1	0.00000	0
15	407.100	407.1	0.00000	0
16	403.712	418.3	0.46153	212.81
17	471.462	434.9	-1.15678	1336.78
18	426.837	463.4	1.15678	1336.85
19	499.688	485.1	-0.46153	212.81
20	271.738	215.9	-1.76662	3117.88
21	454.687	450.0	-0.14831	21.968
22	451.412	456.1	0.14831	21.977
23	409.062	464.9	1.76662	3117.88
24	423.650	464.9	1.30509	1701.56
25	449.225	468.5	0.60983	371.526
26	490.575	471.3	-0.60983	371.5256
27	516.350	475.1	-1.30509	1701.56
28	407.100	407.1	0.00000	0
29	407.100	407.1	0.00000	0

30	407.100	407.1	0.00000	0
31	403.712	418.3	0.46153	212.81
32	471.462	434.9	-1.15678	1336.78
33	426.837	463.4	1.15678	1336.85
34	499.688	485.1	-0.46153	212.81
35	271.738	215.9	-1.76662	3117.88
36	454.687	450.0	-0.14831	21.968
37	451.412	456.1	0.14831	21.977
38	409.062	464.9	1.76662	3117.88
39	423.650	464.9	1.30509	1701.56
40	449.225	468.5	0.60983	371.526
41	490.575	471.3	-0.60983	371.526
42	516.350	475.1	-1.30509	1701.56
43	403.712	418.3	0.46153	212.81
44	471.462	434.9	-1.15678	1336.78
45	426.837	463.4	1.15678	1336.85
46	499.688	485.1	-0.46153	212.81
47	271.738	215.9	-1.76662	3117.88
48	454.687	450.0	-0.14831	21.968
49	451.412	456.1	0.14831	21.977
50	409.062	464.9	1.76662	3117.88
51	423.650	464.9	1.30509	1701.56
52	449.225	468.5	0.60983	371.526
53	490.575	471.3	-0.60983	371.526
54	516.350	475.1	-1.30509	1701.56
				RMSE=31.62

The graphical plot of the predicted BET surface area against the experimental BET surface area is shown in Figure 4.

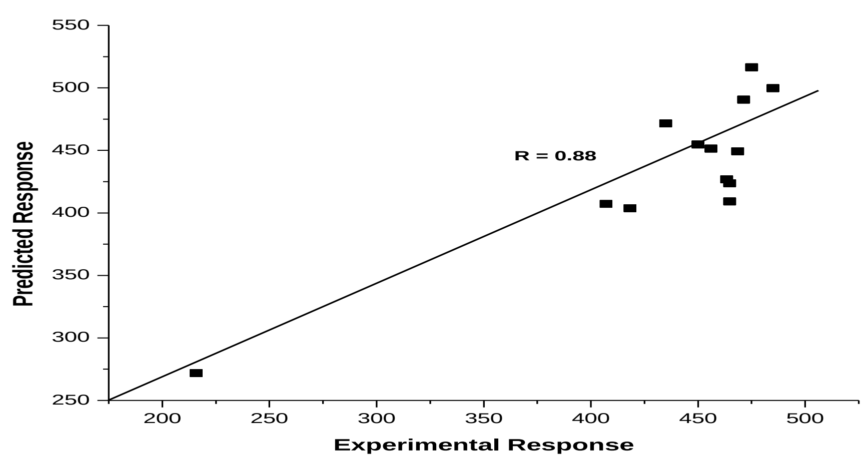

Figure 4: Comparative plot of RSM predicted BET surface area with experimental data.

Figure 4 showed that the data points are randomly distributed about the bisector (45^0) line (non-linear pattern), this indicates that the error residuals for the prediction of the response variable are minimal (normality in data values). Thus, signifying that the response surface model is adequate for response prediction. As well, the relatively high correlation coefficient (R) value of 0.88, confirmed that the response surface model can predict the achievable BET surface area for H2SO4 with reasonable accuracy (Ranade & Ranade., 2023).

The normal plot of residuals shown in Figure 5 was also utilized to check if the process data are normally distributed. The distribution of data points was similar at both the left and right portions of the plot, indicating a normal distribution of the error residuals. This implies that there are no signs of problems with the process data or model (Iheanancho *et al*. 2019).

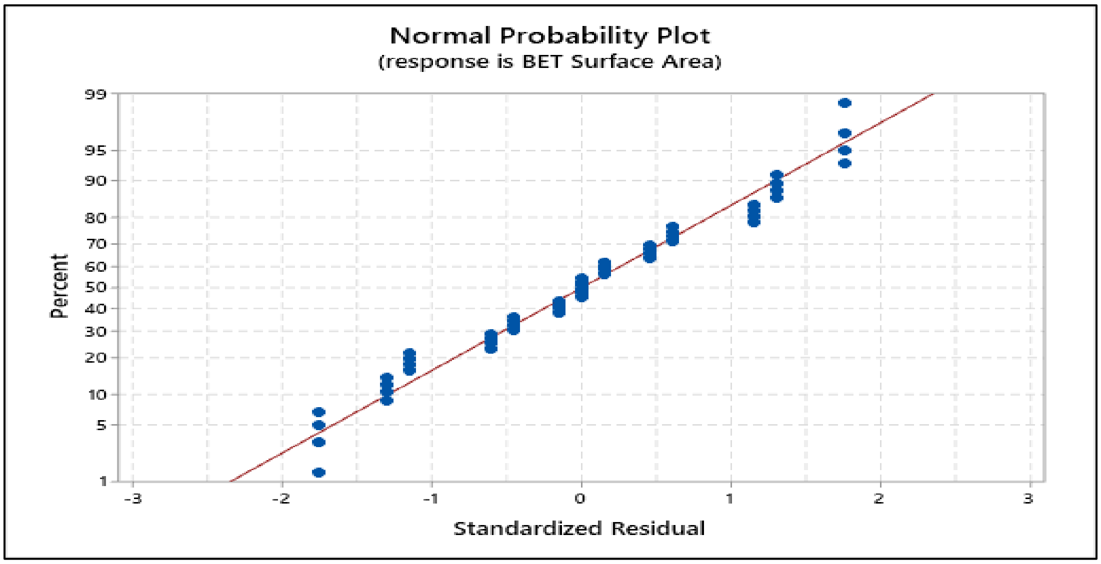

Figure 5: Normal Probability Plot of Residuals for the H2SO4 activated APS.

The statistical significance of the evaluated linear factors, products, and their interactions on the achievable BET surface area (studied response), in order of importance is represented by the Pareto diagram depicted in Figure 6. The vertical continuous line indicates the magnitude of the minimum statistically significant effect for a 95% confidence level and the corresponding t-test value is equal to 2.015. Any factor or its interaction that transcends the vertical line is considered significant (Montgomery, 2017).

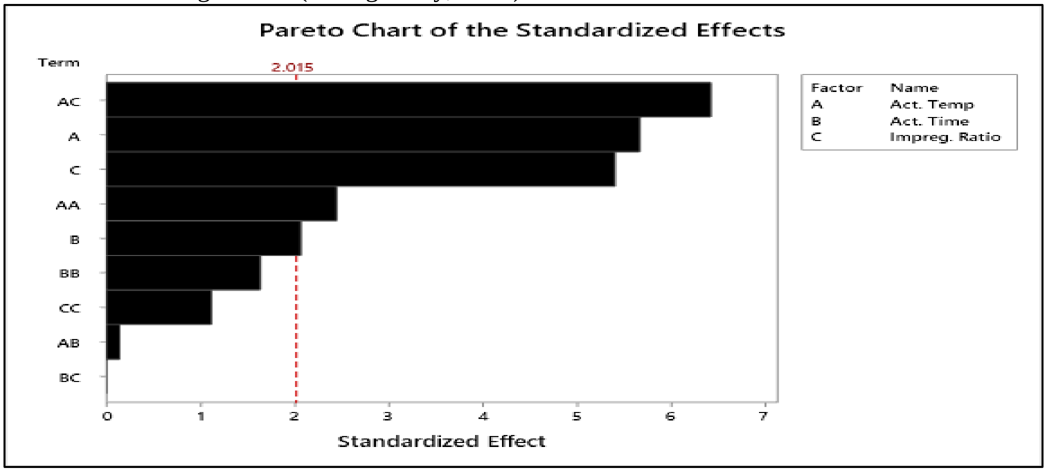

Figure 6: The Pareto plot for H2SO4 activated APS.

Figure 6 shows that the linear effects A (activation temperature), C (impregnation ratio) and the 2-way interaction A*C (activation temperature and impregnation ratio) are the most influential factor determining the achievable surface area of H2SO4-activated APS.

The 3-D response surface plots were created to visualize the relationship between the response (BET surface area) and the independent variables (activation temperature, time, impregnation ratio) in terms of their linear, and interaction effects, and also facilitate optimization of the activated carbon production process are presented in Figure 7(a-c). The quadratic models developed for describing the multivariate system have three independent variables (factors). Hence, each of the response diagrams was plotted as a function of two variables in their respective ranges (-1 to 1), with the other independent variable maintained at zero (0) level.

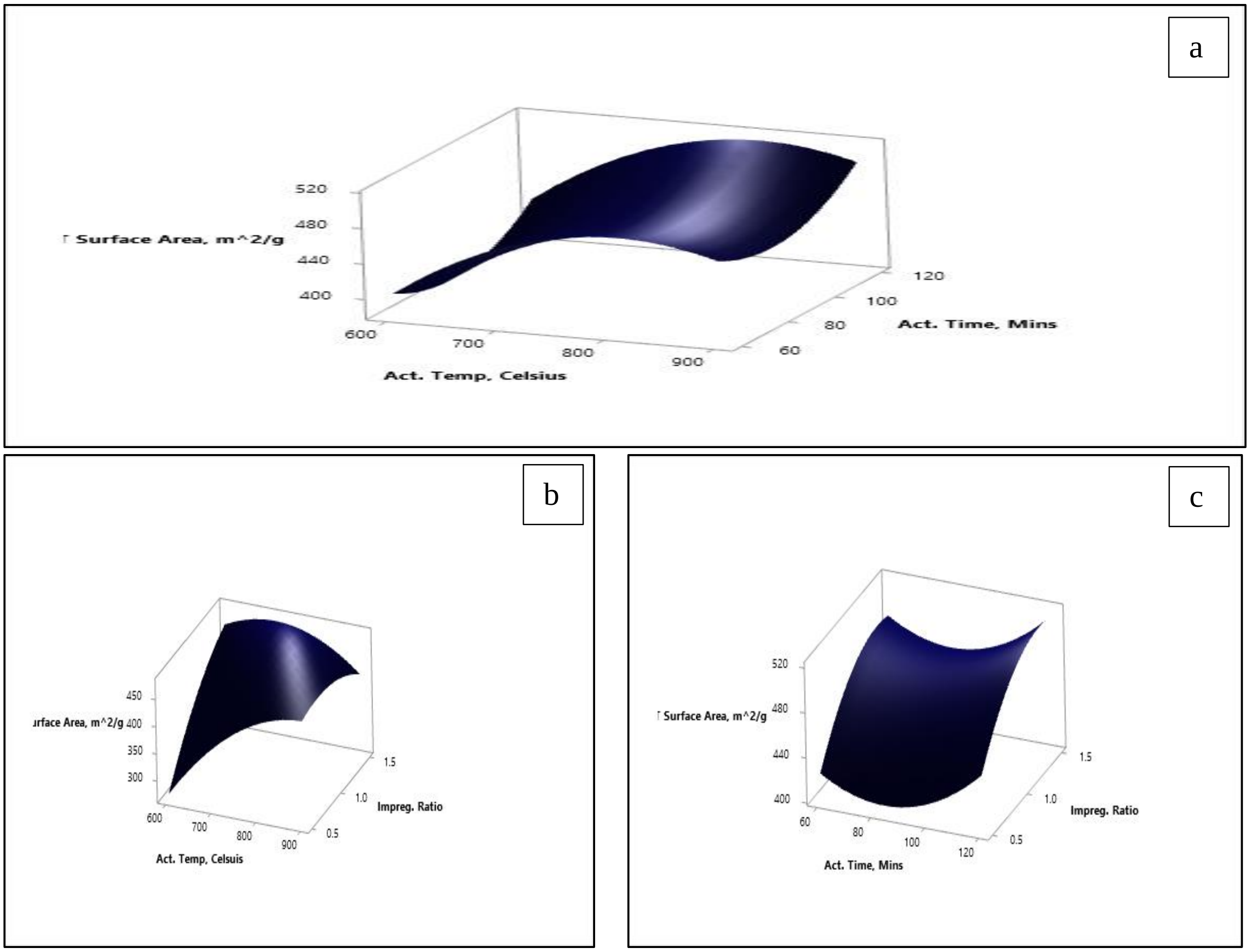

Figure 7: Response surface plots of BET surface area for (a) Impregnation ratio = 1.0 (b) Activation time = 90 mins, and (c) Activation temperature = 750 ^{0}C.

It is apparent from Fig 7a, that the BET surface area of H2SO4 activated carbon showed an increasing trend with increasing activation temperature. Whereas, the achievable BET surface area exhibited an initially decreasing trend with increasing activation time and subsequently, increased to a maximum level. Thus, activation temperature exhibited a synergistic effect on the achievable BET surface area. Here, activation temperature plays a more prominent role in contrast to the extent of activation (activation time) in the activated carbon production process. In Figure 7b, the BET surface area of H2SO4-activated carbon exhibited an increasing trend with increasing activation temperature to a maximum level. On the other hand, BET surface area showed a decreasing trend with increasing impregnation ratio towards a minimum level. It is also evident from Figure 7c, that the BET surface area of H2SO4 activated carbon initially showed a decreasing trend with increasing activation time towards a minimum, subsequently exhibiting an increasing trend for the remainder of the activation process. Conversely, the BET surface area showed an increasing trend with an increasing impregnation ratio towards a maximum value for the duration of the acid activation process. This indicates that the impregnation ratio had a prominent effect on the achievable BET surface area of H2SO4-activated carbon.

From the statistical optimization, the optimum BET surface area achieved for H2SO4-activated avocado pear seeds was 517.8 $m^2.g^{-1}$ for activation temperature of 1045.73K, activation time of 120 mins, and impregnation ratio of 1.21 respectively. Concluding, additional experimental trial run(s) using the optimal conditions were carried out, and the empirical BET surface area for H2SO4-activated APS was found to be 521.26 $m^2.g^{-1}$ (See Table 6). These results validated the second-order polynomial model developed with Response Surface Methodology (RSM).

Table 6: Experimental and predicted value of BET surface area for H2SO4-activated avocado pear seeds utilizing optimum activation conditions.

	Optimal Conditions			BET Surface Area (m^2/g)	
No of Replicates	Activation Time, mins	Activation Temperature, K	Impregnation ratio	Experimental	Predicted
1	120	1045.73	1.21	521.26	517.8

3.2. Modeling of the APS acid activation process using ANN

The ANN BET model was implemented in MATLAB R2018a version 9.4. The accuracy and validity limit of the created ANN BET model for H2SO4-activated APS production process was established by performing diagnostic checks. Standard statistical indices such as correlation coefficient (R), and Root-Mean-square error (RMSE) were utilized to evaluate the ANN BET model performance (Chebii *et al.* 2022; Ranade & Ranade., 2023).

The performance plot of MSE for the number of training cycles for ANN modeling of the HAPS activation process is presented in Figure 8. The overall best validation performance of 64.11 was achieved at 9 iteration cycles through the entire training dataset (Epochs). The relatively low value of the MSE ascertained, indicates that the performance plot did not demonstrate any signs of over-fitting. Moreover, the test (red) and validation (green) curves are comparable, and close to the best fitting curve for this studied case. Consequently, over-fitting problems are not likely to occur with the trained ANN model. However, if the validation curve had exhibited a significantly lower increment in the latter stages of the epochs compared to the test curve in the earlier iteration cycle(s). In this instance, there is the likelihood of occurrence of over-fitting problem(s) (Onu *et al*. 2021).

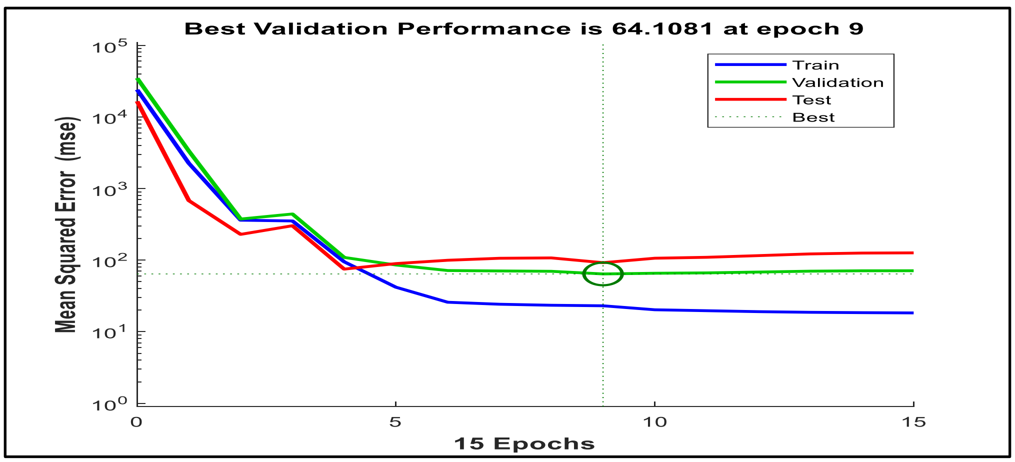

Figure 8: ANN Model Performance chart for HAPS activation process.

The regression plots of preparation, validation, and evaluation are shown in Figure 9 for the ANN BET neural model. The best-fit regression model for HAPS activation corresponded to a correlation coefficient (R) of 0.99764 for training, 0.92419 for testing, and 0.99512 for validation, yielding an average R-value of 0.99552, indicating a strong relationship between the input values and neural network predictions for achievable BET surface area (R_{avg} > 0.995) (Ranade & Ranade., 2023).

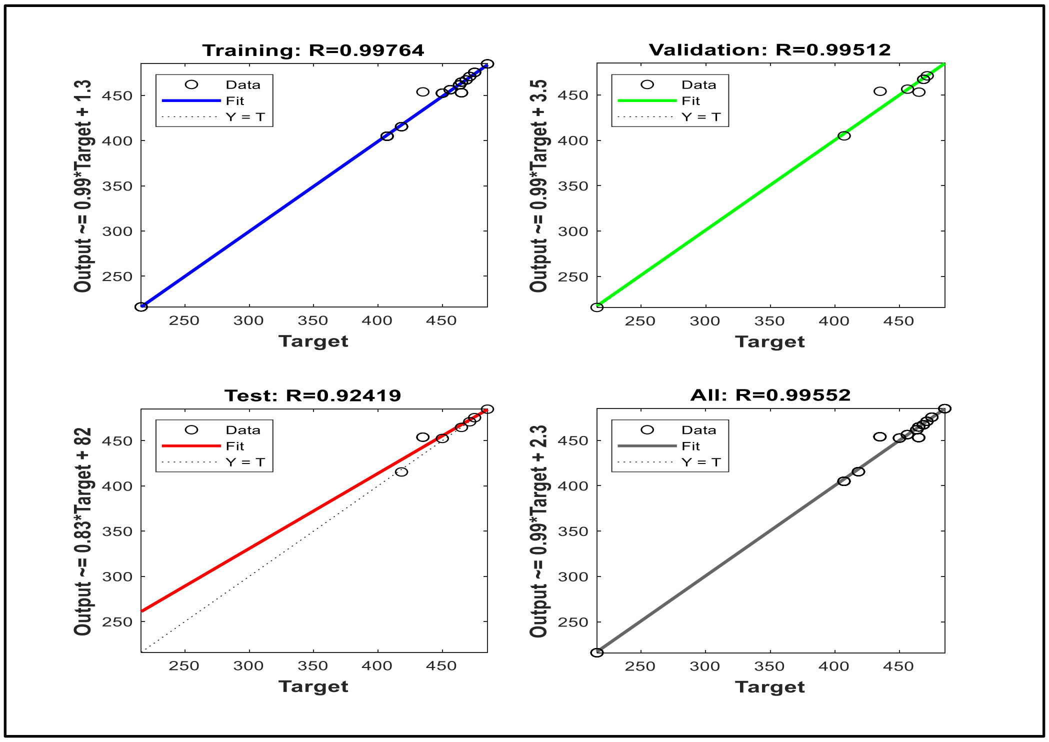

Figure 9: Regression plots for training, validation, testing and overall data for ANN modeling.

To assess the accuracy of the neural models to reproduce the experimental data utilized in network training. The experimentally determined BET surface areas at various activation conditions were compared with ANN-predicted values as shown in Table 7. As expected from the low value of RMSE presented in Table 7, the ANN BET model predicted and experimental results matched very well (6.25). The low value of RMSE obtained shows that the hidden layers (levels) of the ANN neural network were able to decipher the pattern of training, resulting in better model prediction performance (Chebii *et al.* 2022). This indicates that the ANN BET model can accurately replicate the experimental results for the APS acid activation process.

Table 7: Comparison of ANN outputs with experimental observations for production of H_2SO_4- activated APS.

Point	BET Surface Area m^2/g (ANN)	BET Surface Area m^2/g (Experiment)	Residual Square
1	415.42	418.3	8.3214
2	453.90	434.9	360.875
3	461.65	463.4	3.0645
4	484.87	485.1	0.0530
5	216.01	215.9	0.0112
6	452.67	450	6.0864
7	456.275	456.1	0.03055
8	464.70	464.9	0.0391
9	452.96	464.9	142.611
10	467.06	468.5	2.0715
11	470.93	471.3	0.1368
12	475.46	475.1	0.1290
13	404.85	407.1	5.05762
14	404.85	407.1	5.0576
15	404.85	407.1	5.0576

16	415.42	418.3	8.3214
17	453.90	434.9	360.875
18	461.65	463.4	3.0645
19	484.87	485.1	0.0530
20	216.01	215.9	0.0112
21	452.47	450	6.0864
22	456.27	456.1	0.03055
23	464.70	464.9	0.03906
24	452.96	464.9	142.611
25	467.061	468.5	2.07148
26	470.93	471.3	0.13679
27	475.46	475.1	0.12905
28	404.85	407.1	5.05762
29	404.85	407.1	5.05762
30	404.85	407.1	5.05762
31	415.42	418.3	8.3214
32	453.90	434.9	360.8751
33	461.65	463.4	3.06446
34	484.87	485.1	0.052954
35	216.01	215.9	0.0112
36	452.47	450	6.08644
37	456.27	456.1	0.03055
38	464.70	464.9	0.039056
39	452.96	464.9	142.611
40	467.06	468.5	2.07148
41	470.93	471.3	0.136790
42	475.46	475.1	0.129045
43	415.42	418.3	8.3214
44	453.90	434.9	360.875
45	461.65	463.4	3.06446
46	484.87	485.1	0.05295
47	216.01	215.9	0.0112
48	452.47	450	6.08644
49	456.27	456.1	0.03055
50	464.70	464.9	0.03906
51	452.96	464.9	142.610
52	467.06	468.5	2.0715
53	470.93	471.3	0.1368
54	475.46	475.1	0.1290
			RMSE = 6.25

Furthermore, the ANN BET model was examined by comparing the ANN predictions and experimental outcomes for achievable surface area(s), as presented in Figure 10.

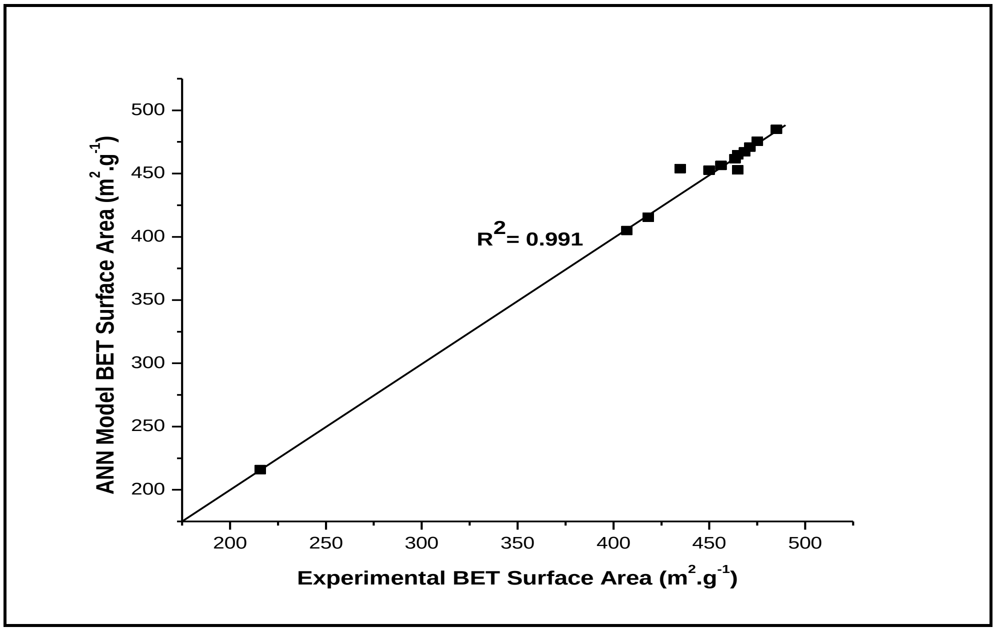

Figure 10: Parity plot of ANN model predicted and experimental results for the HAPS activation process.

As apparent from Figure 10, the ANN predicted values and experimental results are in good agreement, as indicated by the high R^2 value of 0.991. $R^2 > 0.67$ is an indicator of the high predictive accuracy of the non-linear regression model (Singh *et al.* 2014). Thus, the neural network model was able to discern the pattern of activation parameters to provide an accurate prediction of periodic variations in the achievable BET surface area(s) of HAPS.

3.3. Comparative Analysis of RSM and ANN BET models

The prediction accuracy of the response surface (RS) and artificial neural network (ANN) BET models was compared, employing performance indices-Root mean square error (RMSE), Correlation coefficient (R) and Squared loss function as reported in Table 8. The statistical index-squared loss function better reveals model performances because it is non-negative, and very sensitive to outliers at the individual data points (Gokcesu & Gokcesu., 2023).

Table 8: Comparison of RSM and ANN BET models for activation of HAPS.

Run No	RSM Square residual	ANN Square residual
1	212.81	8.3214
2	1336.78	360.875
3	1336.85	3.0645
4	212.81	0.0530
5	3117.88	0.0112
6	21.968	6.0864
7	21.977	0.03055
8	3117.88	0.0391
9	1701.56	142.611
10	371.53	2.0715
11	371.53	0.1368
12	1701.56	0.1290
13	0	5.05762
14	0	5.0576
15	0	5.0576

16	212.81	8.3214
17	1336.78	360.875
18	1336.85	3.0645
19	212.81	0.0530
20	3117.88	0.0112
21	21.968	6.0864
22	21.977	0.03055
23	3117.88	0.03906
24	1701.56	142.611
25	371.526	2.07148
26	371.5256	0.13679
27	1701.56	0.12905
28	0	5.05762
29	0	5.05762
30	0	5.05762
31	212.81	8.3214
32	1336.78	360.8751
33	1336.85	3.06446
34	212.81	0.052954
35	3117.88	0.0112
36	21.968	6.08644
37	21.977	0.03055
38	3117.88	0.039056
39	1701.56	142.611
40	371.526	2.07148
41	371.526	0.136790
42	1701.56	0.129045
43	212.81	8.3214
44	1336.78	360.875
45	1336.85	3.06446
46	212.81	0.05295
47	3117.88	0.0112
48	21.968	6.08644
49	21.977	0.03055
50	3117.88	0.03906
51	1701.56	142.610
52	371.526	2.0715
53	371.526	0.1368
54	1701.56	0.1290
	RMSE= 31.62	**RMSE** = 6.25

RSM and ANN BET models have squared-error residual values ranging from 21.98 to 3117.88, and 1.12×10^{-2} to 360.88 respectively for achievable BET surface area(s). The lower squared-error residual values obtained for the ANN model indicate that the model has better predictive performance than RSM. Further, The RSM and ANN BET models generated correlation coefficient (R) values of 0.88 and 0.9955 respectively for achievable BET surface area(s). The higher value of the regression coefficient determined for ANN BET model indicated that the ANN performed better than RSM. In addition, Figure 11 showed relatively low Root Mean Squared Error (RMSE) values of 6.25 and 31.62 for the ANN and RSM models respectively in this studied case. RMSE is also a standard statistical index for evaluating the performance of non-linear regression models (Chebii *et al.* 2022).

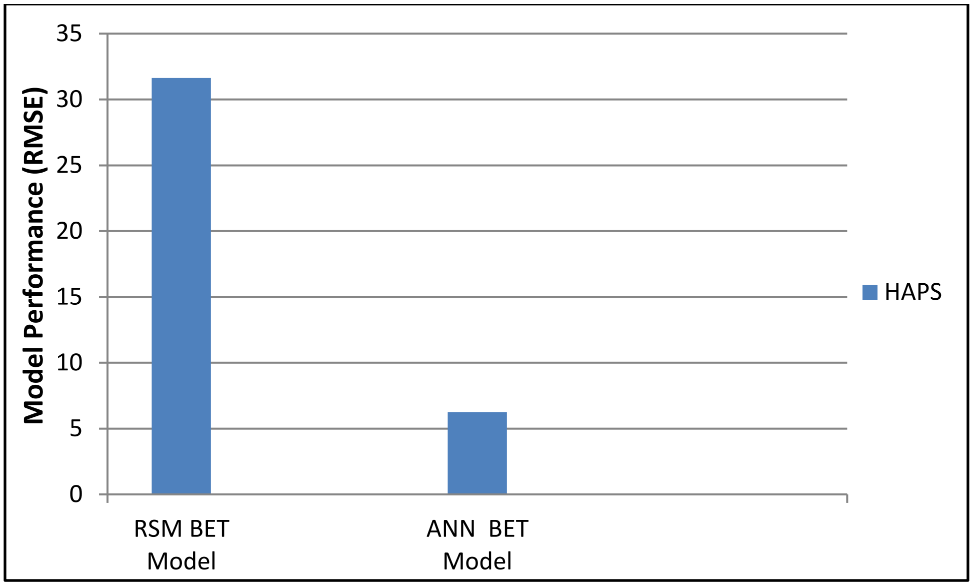

Figure 11: Model BET prediction performances for HAPS activation process.

These results confirm that the ANN model is the most capable model for predicting the achievable surface area of H2SO4-activated APS. These results are in agreement with findings made by Nazerian *et al.* (2018) and Nur *et al*. (2019), which reported that ANN analysis performed better than RSM in prognostic ability. In a nutshell, ANN and RSM techniques have been proven to be effective methods for predicting and forecasting the achievable BET surface area of H2SO4-activated Avocado Pear Seeds (APS) produced under varied activation conditions in a muffle furnace.

4.0. Conclusion

In this study, Response Surface Methodology (RSM) utilizing Box Behnken Design (BBD) and ANN of Machine learning (ML) technology were employed to explore the effects of independent variables on the response variable and optimize the process conditions for the production of avocado pear seed activated carbons using H_2SO_4. The effectiveness of RSM and ANN techniques for optimization of the process conditions for preparation of H2SO4 activated avocado pear seed carbons having maximal BET surface area(s) was successfully demonstrated. The RSM and ANN BET models obtained via non-linear regression analysis predicted the response variable ((BET surface area) from the experimental dataset to a reasonable degree of accuracy. The RSM optimization concluded that the most influential parameter in achievable BET surface area for H2SO4-activated avocado pear seed (APS) was activation temperature. The maximum BET surface area for H2SO4-activated APS obtained from RSM optimization, and subsequently verified via additional experimental trials was estimated to be 517.8 $m^2.g^{-1}$ achievable at optimum conditions of activation temperature (1045.73 K), activation time (120 mins), and Impregnation ratio (1.21). Error analysis conducted between simulated and experimental values using various statistical indices (correlation coefficient, root mean square error and squared loss function) for both the RSM (BBD) and ANN models, confirmed that ANN has better prognostic performance. In conclusion, the H2SO4-acid-activation of pristine avocado pear seeds has good potential to produce quality active carbons possessing high BET surface area.

References

Ajemba, R. O., 2012. *Thermodynamics and kinetic modeling of the dissolution and adsorptive applications of Ukpor, Udi, and Nteje clays*. PhD Dissertation, Nnamdi Azikiwe University.

Ali, R.A., Hamad, H.A., Hussien, M.H. & Malash, G.F. 2016. Potential of using green adsorbent of heavy metal removal from aqueous solutions: Adsorption kinetics, isotherm, thermodynamics, mechanism and economic analysis. *Ecological Engineering*. 91: 317-332.

Anderson & Whitcomb. 2016. *RSM Simplified*. 2nd Ed. New York: Productivity Inc.

Basu, P. 2013. *Biomass gasification, pyrolysis, and torrefaction: Practical design and theory*. Amsterdam: Academic Press.

Bhowmik, K.L., Debnath, A., Nath, R.K., Das, S, Chattopadhyay, K.K. & Saha, B. 2016. Synthesis and characterization of mixed phase manganese ferrite and hausmannite magnetic nanoparticle as potential adsorbent for methyl orange from aqueous media: artificial neural network modeling. *Journal of Molecular Liquids*. 219: 1010-1022.

Bodzek, M., Konieczny, K. & Kwiecinska-Mydlak, A. 2020. Nanotechnology in water and wastewater treatment. Graphene-the nanomaterial for next generation of semipermeable membranes. *Critical reviews in Environmental Science and Technology*. 50: 1515-1579.

Buasri, A., Sirikoom, P., Pattane, S., Buachum, O. & Loryuenyong, V. 2023. Process Optimization of Biodiesel from Used Cooking Oil in a Microwave Reactor: A Case of Machine Learning and Box–Behnken Design. *ChemEngineering*, 7(4), 65.

Chebii, S. J., Mukolwe, M. M. & Ong'or, B. I. 2022. River flow modelling for flood prediction using artificial neural network in ungauged Perkerra catchment, Baringo County, Kenya. *Water Practice and Technology*, 17(4): 914-929.

Gokcesu, K. & Gokcesu, H. 2023. *A Note On Nonlinear Regression Under L2 Loss*. Available from: https://doi.org/10.48550/ARXIV.2303.17745/. [13 February 2024].

Goswami, L., Pakshirajan, K. & Pugazhenthi, G. 2020. Biological treatment of biomass gasification wastewater using hydrocarbonoclastic bacterium Rhodococcus opacus in an up-flow packed bed bioreactor with a novel waste-derived nano-biochar based bio-support material. *Journal of Cleaner Production*, 256: 120-253.

Howard, S.P., Rowe, D. R. & Tchobanogolous, G. 1986. *Environmental Engineering*. Singapore: McGraw-Hill.

Ighalo, O.J., Yao. B, Zhou, Z.Y. & Rangabhashiyam, S. 2022.'Utilization of avocado (Persea americana) adsorbents for the elimination of pollutants from water: a review'. *In book:Biomass-Derived Materials for Environmental Applications*. Netherlands: Elsevier.

Iheanacho, C.O., Nwabanne, J.T. & Onu, C.E. 2019. Optimum process parameters for activated carbon production from rice husk for phenol adsorption. *Current Journal of Applied Science and Technology*. 36 (6): 1–11.

Jafarinejad, S. 2017. Environmental Impacts of the Petroleum Industry, Protection Options, and Regulations. In *Petroleum Waste Treatment and Pollution Control*. Netherlands: Elsevier: 85-116.

Li, R. Y. M., Fong, S. & Chong, K. W. S. 2017. Forecasting the REITs and stock indices: Group Method of Data Handling Neural Network approach. *Pacific Rim Property Research Journal*, 23(2): 123-160.

Malik, D. S., Jain, C. K. & Yadav, A. K. 2017. Removal of heavy metals from emerging cellulosic low-cost adsorbents: A review. *Applied Water Science*, 7(5): 2113–2136.

Marsh, H. & Rodríguez-Reinoso, F. 2006. *Activated carbon*. Netherlands: Elsevier.

Mohammad, Y.S., Shaibu-Imodagbe, E.M., Igboro, S.B., Giwa, A., Okuofu. & C.A. 2014. Modeling and optimization for production of rice husk activated carbon and adsorption of phenol. *Journal of Engineering*: 1-10.

McCulloch, W.S. & Walter., P. 1943. A logical calculus of the ideas immanent in nervous activity. *Bulletin of Mathematical Biophysics*. Vol 5.

Melvin, S. S., Abigail, M. E. A. & Chidambaram, R. 2015. Isotherm modelling , kinetic study and optimization of batch Parameters using response surface methodology for effective removal of Cr (VI) using fungal biomass. *PLOS One*, 10(3): 1-13.6

Montgomery, D.C. 2017. *Design and Analysis of Experiments*. New Jersey: John Wiley and Sons.

Müller, A., Österlund, H., Marsalek, J. & Viklander, M. 2020. The pollution conveyed by urban runoff: A review of sources. *Science of The Total Environment*, 709: 136125.

Nazerian, M., Kamyabb, M., Shamsianb, M., Dahmardehb. & M., Kooshaa, M. 2018. Comparison of response surface methodology (RSM) and artificial neural networks (ANN) towards efficient optimization of flexural properties of gypsum-bonded fiberboards. *CERNE*, 24(1): 35-47.

Nooshin, A. & Hamid, Z. 2017. Optimization of organosolv pretreatment of rice straw for enhanced biohydrogen production using Enterobacter aerogenes. *Bioresource Technology*, 227, :335-344.

Nur, S.R.T., Mohd, I.E.H., Siti, S.A.G., Uswatun, H.Z. & Mohd, Y.A.S. 2019. Artificial neural networks (ANNs) and response surface methodology (RSM) approach for modelling the optimization of chromium (vi) reduction by newly isolated acinetobacter radioresistens strain ns-mie from agricultural soil. *Hindawi Biochemistry and Medical Research International*: 1-14.

Okpe, E.C., Asadu, C.O. & Onu, C.E. 2018. Statistical analysis for orange G adsorption using kola nut shell activated carbon. *Journal of the Chinese Advanced Materials Society*: 1-15.

Okewale, A. O., Igbokwe, P. K. & Adesina, O. A. 2015. Optimization of the adsorptive dehydration of ethanol-water system. *Chemical and Process Engineering Research*, 39(3): 27-37.

Onu, C. E., Nwabanne, J.T., Ohale, P.E. & Asadu., C.O. 2021. Comparative Analysis of RSM, ANN and ANFIS and the mechanistic modeling in eirochrome black-T dye adsorption using Modified clay. *South African Journal of Chemical Engineering*. 36: 24-42.

Ranade, N. V. & Ranade, V. V. 2023. ANN based surrogate model for key Physico-chemical effects of cavitation. *Ultrasonics Sonochemistry*, 94: 106-327.

Singh, S.K, Jain, S.K. & Bardossy, A. 2014. Training of artificial neural network using information rich data. *Hydrology*.pp. 40-62.

Suzuki, M. 1990. *Adsorption engineering*. Netherlands: Elsevier.

Van Dyk, L. D. 2000. *The Production of Granular Activated Carbon from Agricultural Waste Products*. Master's Thesis, Stellenbosch University.

Yang, X., Wan, Y., Zheng, Y., He, F., Yu, Z., Huang, J., Wang, H., Ok, Y. S., Jiang, Y. & Gao, B. 2021. Surface functional groups of carbon-based adsorbents and their roles in the removal of heavy metals from aqueous solutions: A critical review. *Chemical Engineering Journal*, 366 :608-621.

Zarzour, M., Ensafi, A.A. & Rezaei, B. 2014. Preparation of activated carbon from organic fraction of municipal solid wastes by $ZnCL_2$ activation method and its use for elimination of chromium(vi) from aqueous solutions. *Journal of the Iranian Chemical Society*, 11(4): p.3

Zhu, Y., Kolar, P., Shah, S. B., Cheng, J. J. & Lim, P. K. 2016. Avocado seed-derived activated carbon for mitigation of aqueous ammonium. *Industrial Crops and Products*, 92: 34-41.